Inorganic Chemistry

Article

pubs.acs.org/IC

Electrophilic Alkylation of Pseudotetrahedral Nickel(II) Arylthiolate Complexes

Tapash Deb and Michael P. Jensen*

Department of Chemistry and Biochemistry, Ohio University, Athens, Ohio 45701, United States

Supporting Information

ABSTRACT: A kinetic study is reported for reactions of pseudotetrahedral nickel(II) arylthiolate complexes [($Tp^{R,Me}$)Ni−SAr] ($Tp^{R,Me}$ = hydrotris{3-R-5-methyl-1-pyrazolyl}borate, R = Me, Ph, and Ar = C_6H_5, C_6H_4-4-Cl, C_6H_4-4-Me, C_6H_4-4-OMe, 2,4,6-$Me_3C_6H_2$, 2,4,6-$^iPr_3C_6H_2$) with organic electrophiles R′X (i.e., MeI, EtI, BzBr) in low-polarity organic solvents (toluene, THF, chloroform, dichloromethane, or 1,2-dichloroethane), yielding a pseudotetrahedral halide complex [($Tp^{R,Me}$)Ni−X] (X = Cl, Br, I) and the corresponding organosulfide R′SAr. Competitive reactions with halogenated solvents and adventitious air were also examined. Akin to reactions of analogous and biomimetic zinc complexes, a pertinent mechanistic question is the nature of the reactive nucleophile, either an intact thiolate complex or a free arylthiolate resulting from a dissociative pre-equilibrium. The observed kinetics conformed to a second-order rate law, first order with respect to the complex and electrophile, and no intermediate complexes were observed. In the absence of a mechanistically diagnostic rate law, a variety of mechanistic probes were examined, including kinetic effects of varying the metal, solvent, electrophile, and temperature, as well as the 3-pyrazolyl and arylthiolate substituents. Compared to zinc analogues, the effect of Ni−SAr covalency is also of interest herein. The results are broadly interpreted with respect to the disparate mechanistic pathways.

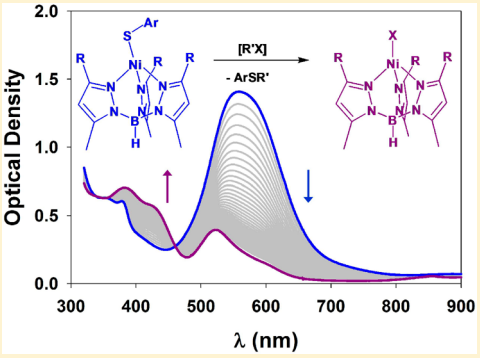

1. INTRODUCTION

Metal−thiolate (M−SR) bonds are a ubiquitous and essential feature of many diverse metalloenzyme active sites.[1] Several prominent examples include heme iron-dependent cytochrome P450,[2] non-heme iron-dependent superoxide reductase,[3−5] iron- and cobalt-dependent nitrile hydratases,[6] thiolatocobalamins,[7] Fe/Ni-hydrogenase,[8] nickel-dependent superoxide dismutase,[3] acetyl-coenzyme A synthase[9] and methyl-coenzyme M reductase,[10] Type I copper and Cu_A redox centers,[11] and zinc-dependent methyltransferase enzymes[12] such as methionine synthase,[13] as well as the Ada DNA repair protein.[14] M−SR bonds support a rich array of biological reactivity, including alkylation,[15] protonation,[16] oxidation,[17] and oxygenation.[18]

Zinc-mediated biological alkyl group transfer has been extensively modeled by electrophilic alkylation of synthetic complexes.[19] Several classes of zinc complexes have been studied, including tetrahedral homoleptic arylthiolate adducts,[20,21] square-pyramidal complexes with macrocyclic supporting ligands,[22,23] pseudotetrahedral complexes supported by hydrotris(pyrazolyl)borate[24] ligands [(Tp)Zn−SR] and related facially tridentate "scorpionate" ligands,[25−34] as well as complexes of polydentate ligands with incorporated thiolate donors.[33−36]

Two limiting alkylation mechanisms have been proposed that involve distinct nucleophiles:[37] predissociation of strongly nucleophilic free thiolate (Scheme 1, pathway A)[21,22,32,38] and an associative reaction of intact thiolate complexes. The associative mechanism may proceed by distinct pathways: either by a four-centered transition state (i.e., σ-bond metathesis, pathway B) or by a classical S_N2 mechanism (pathway C).[37] Relative to the dissociative and associative S_N2 pathways, the reaction barrier for σ-bond metathesis was calculated to be intrinsically unfavorable for several computational NS_2 heteroscorpionate models,[37] although an additional possibility germane to scorpionate complexes is that of anchimeric assistance involving donor arm dechelation.[28]

An associative reaction will exhibit overall second-order kinetics, rigorously first order with respect to both the complex and nucleophile.[39] The kinetics of a reversible dissociative mechanism are more complicated; first-order behavior with respect to the complex is obtained under pre-equilibrium or steady-state conditions,[39] whereas the order with respect to the electrophile would range from first-order at low concentrations where alkylation is rate-limiting toward a zero-order limit where thiolate dissociation is rate-limiting. Although observation of saturating kinetics with respect to electrophile concentration would be consistent with reversible thiolate dissociation, second-order kinetics are not sufficient to distinguish the mechanism.[30] The associative S_N2 pathway would be distinguished by a diagnostic organosulfide complex intermediate (Scheme 1, top right), but the organosulfide ligand is rapidly displaced from substitution-labile metal ions by the leaving group (i.e., X^-).[26,32−35]

Received: July 29, 2014
Published: December 15, 2014

   dx.doi.org/10.1021/ic5018328 | Inorg. Chem. 2015, 54, 87−96

Scheme 1

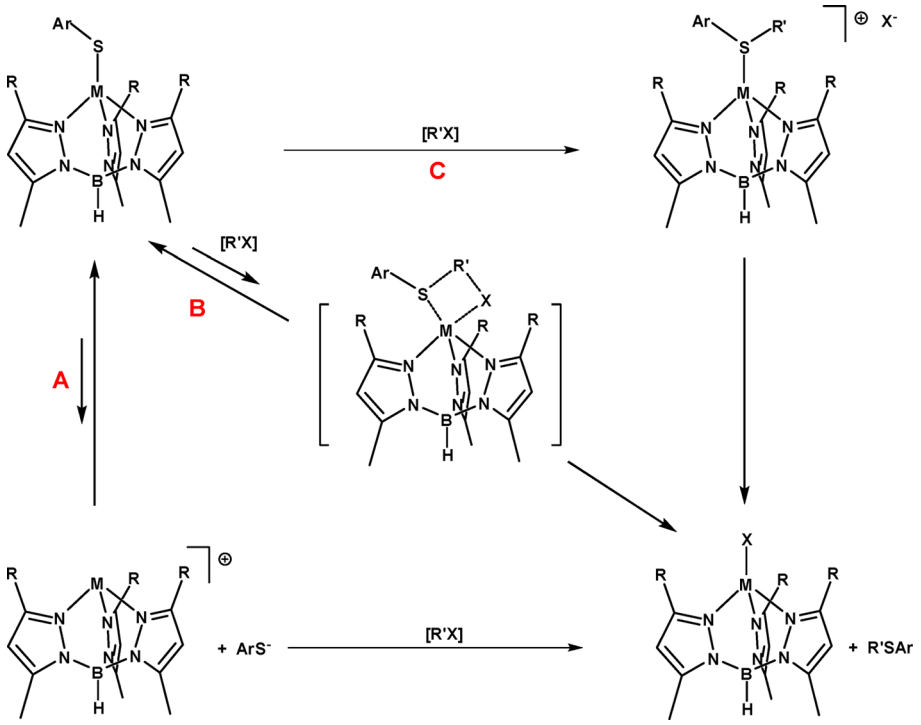

A prototypical kinetic study of $(MeO)_3P{=}O$ demethylation in DMSO solution by a series of arylthiolate complexes $[NMe_4]_{2-n}[Zn(SPh)_{4-n}(1\text{-methylimidazole})_n]$ (n = 0, 1, 2) found that reactivity increased with the anionic charge of the complexes: $[Zn(SPh)_2(MeIm)_2]$ < $[Zn(SPh)_3(MeIm)]^-$ < $[Zn(SPh)_4]^{2-}$.[20,21] The observed second-order rate constant of the homoleptic dianion approaches that of free phenylthiolate, and ^{1}H NMR line broadening provided evidence for facile thiolate dissociation and exchange. A dissociative equilibrium was proposed for $[Zn(SPh)_4]^{2-}$, with subsequent alkylation of the free arylthiolate anion; the kinetic data were fit according to this model.[21]

In contrast, alkylation of the substitution-inert organometallic complexes $[CpFe(CO)_2SR]$ (Cp = η^5-C_5H_5 and R = Me, Et, Ph) with the potent electrophile MeI proceeds by an associative mechanism in DMSO or acetone solutions. Second-order kinetics were observed, as well as metastable thioether complex intermediate salts $[CpFe(CO)_2(MeSR)]^+(I^-)$;[40−42] under more vigorous conditions, subsequent ligand substitution occurs to give $[CpFe(CO)_2I]$ and free organosulfide MeSR as the final products.[40] Redox chemistry is also possible for iron(II), but no evidence was found for complex oxidation or free radical formation.[40]

Mechanistic assignment for reactivity of neutral scorpionate complexes (e.g., [(Tp)Zn−SR]) with strong organic electrophiles (e.g., MeI, BzBr) in low-polarity solvents is more challenging.[25−34] Overall second-order behavior is typically observed,[25] usually under pseudo-first-order conditions with excess electrophile.[26−28,30−32] Observed rates are much slower than that of free thiolate anion,[32] organosulfide complexes are not observed,[25−28,31,32] and exchange reactions with free thiolate salts are relatively slow for $[(Tp^{Ph,Me})Zn{-}SR]$ in chloroform and DMSO.[26,43] Therefore, an associative mechanism is frequently invoked.[25−28,31,32] On the other hand, the assignment of an associative mechanism has been questioned in some instances.[28,30,35] Facile thiolate exchange has been reported for other scorpionates;[32,44] in one such case, that of a sulfur-rich hydrotris(2-mercapto-imidazolyl)borato scorpionate incorporating an intramolecular hydrogen bond to the thiolate sulfur, a dissociative mechanism was assigned for reaction with MeI in chloroform on the basis of rapid thiolate exchange and observed kinetic isotope effects.[30,44]

The reactivity of transition metal analogues is of interest with respect to the enhanced covalency of M−SR bonding, as influenced by disparate ligand field geometries, variable d electron counts, and accessible spin states.[45] Kinetic studies have been reported for reactions of neutral square-planar and cationic square-pyramidal nickel(II) complexes with various organic electrophiles,[22,36,46,47] but pseudotetrahedral scorpionate complexes have not been examined in any detail.[45,48−54] Because a common pseudotetrahedral geometry and a significant ionic component are retained in M−SAr bonding,[45] the mechanistic discussion of the zinc(II) complexes (Scheme 1) is also relevant for nickel(II) analogues, although alternative redox mechanisms are possible.[46]

We recently prepared and characterized a number of such arylthiolate complexes $[(Tp^{R,Me})Ni{-}SAr]$ (R = Me, Ph).[51−53] A key feature of these complexes is the steric interaction between the arylthiolate substituent and the proximal 3-pyrazole substituents,[24,28] which leads to significant structural effects.[49−54] Moreover, electronic properties of the arylthiolate are readily manipulated. A preliminary demonstration of electrophilic alkylation by MeI (Ar = Ph and Mes, 2,4,6-$Me_3C_6H_2$) revealed a second-order rate law.[51] In the present work, additional insights into the relevant alkylation mechanism were sought using a suite of kinetic and extrakinetic probes of mechanism,[39] including Arrhenius and Hammett analyses, as well as the elucidation of solvent, substituent, and conformational effects.

dx.doi.org/10.1021/ic5018328 | Inorg. Chem. 2015, 54, 87−96

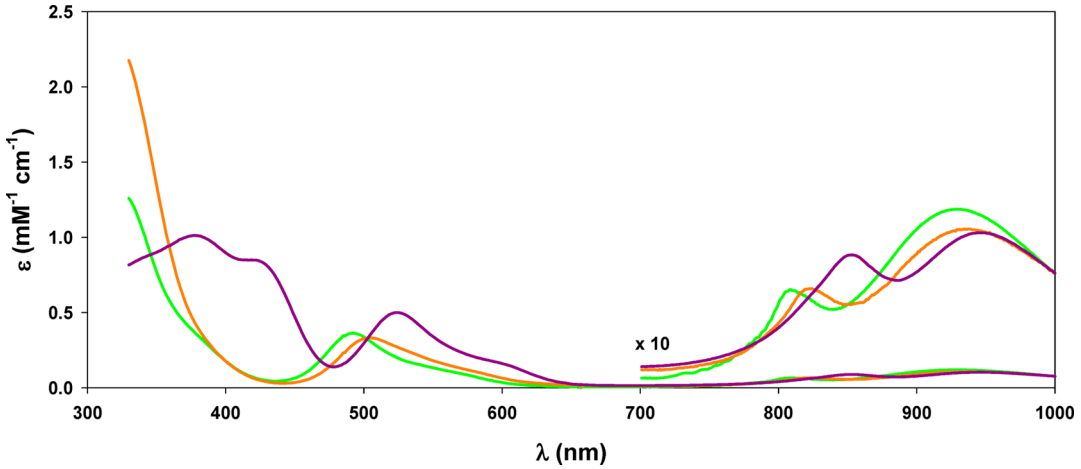

Figure 1. UV−vis−NIR spectra of authentic [(Tp^{Ph,Me})Ni−X] (X = Cl (green), Br (orange), I (violet)) in 1,2-dichloroethane at 298 K, with 10-fold vertical expansion from 700 to 1000 nm.[56]

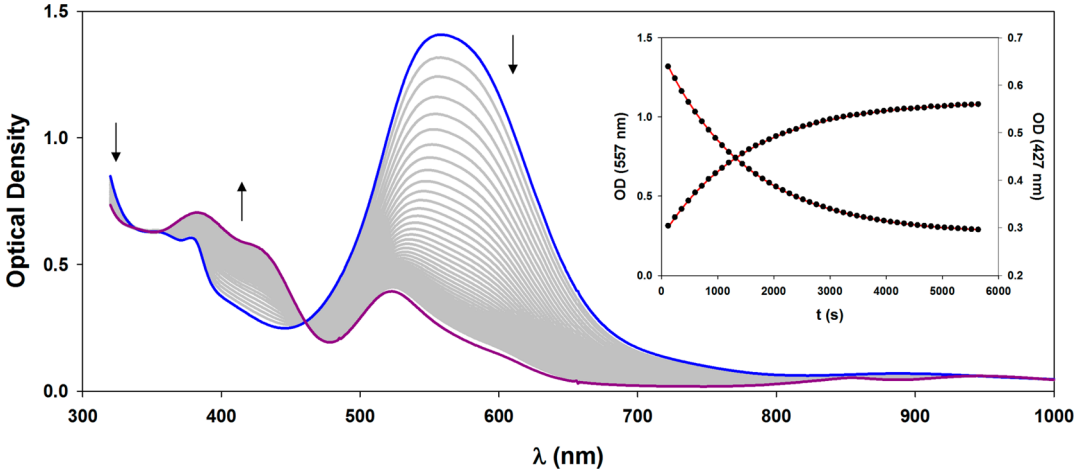

Figure 2. Time-dependent UV−vis−NIR spectra (gray) for the reaction of [(Tp^{Ph,Me})Ni−SMes] with MeI (78 mM) in 1,2-dichloroethane at 326.2 K with limiting spectra (blue, violet) obtained from a global fit (k_{obs} = 6.64(1) × 10^{-4} s^{-1}). Inset shows single-wavelength exponential fits for decay of [(Tp^{Ph,Me})Ni−SMes] observed at 557 nm (k_{obs} = 6.59(1) × 10^{-4} s^{-1}; r^2 = 1.00) and accumulation of [(Tp^{Ph,Me})Ni−I] observed at 427 nm (k_{obs} = 6.63(2) × 10^{-4} s^{-1}; r^2 = 1.00).

2. EXPERIMENTAL SECTION

The synthesis and characterization of all thiolate complexes [(Tp^{R,Me})-Ni−SAr] (R = Me, Ph)[51−54] utilized herein, as well as the halide product complexes [(Tp^{R,Me})Ni−X] (R = Me,[55] Ph;[56] X = Cl, Br, I), were reported previously. All reaction solutions were prepared under argon in a glovebox (MBraun Unilab), loaded into cuvettes, and sealed under a rubber septum with a threaded screw cap (Starna, Atascadero, CA). Control solutions were oxygenated as previously described[57] by brief bubbling with O_2 gas predried by passage through a bed of $MgSO_4$ and CaH_2. Time-dependent UV−vis−NIR spectra were recorded on an Agilent HP-8453 diode-array spectrophotometer using a jacketed cuvette holder interfaced to a circulating bath equipped with heating and cooling elements under control of a thermostat (VWR). Multivariate nonlinear least-squares fits were calculated for time-dependent UV−vis−NIR spectra using SPECFIT/32.[58,59] Observed rates of electrophilic alkylations are listed in Table S1 in the Supporting Information (SI). Alternative single-wavelength exponential fits were calculated by nonlinear least-squares regression using SigmaPlot 8.02 (SPSS, Inc.).[60] Gas chromatography−mass spectrometry (GC−MS) data were obtained on a Shimadzu QP2010 SE instrument after passage of reaction solutions through a silica plug to remove inorganic components; the initial column temperature of 50 °C was increased by 12 °C/min to 210 °C and then 15 °C/min to 315 °C.

3. RESULTS AND DISCUSSION

3.1. General Remarks Regarding the Reactivity of [(Tp^{R,Me})Ni−SAr] with Electrophiles. The arylthiolate complexes [(Tp^{R,Me})Ni−SAr] (R = Me, Ph) react with organic electrophiles (R′X = MeI, EtI, BzBr, $ClCH_2CH_2Cl$) to form the corresponding halide complex [(Tp^{R,Me})Ni−X] (Figure 1) and free organosulfide R′SAr (eq 1). Decompositions of [(Tp^{R,Me})-Ni−SAr] were monitored by time-dependent UV−vis−NIR spectroscopy (Figure 2), and observed kinetics conformed to an overall second-order rate law (eq 2). Values of k_0 and k_1 were extracted from the observed rate (k_{obs}) by variation of electrophile concentration (i.e., $[R'X]_0$, eq 3) under pseudo-first-order conditions. A preliminary demonstration of [(Tp^{R,Me})Ni−SAr] alkylation with MeI in CH_2Cl_2 solutions revealed a small positive intercept at 297 K (i.e., $k_0 > 0$), which was speculatively assigned to rate-limiting thiolate dissociation under saturating $[MeI]_0$.[51] The more extensive investigation herein shows that k_0 actually reflects a composite of minor side reactions with halogenated solvent (eq 4) and adventitious air (eq 5 and/or eq 6), as well as any systematic error in determining $[MeI]_0$ (section 3.8, SI).

dx.doi.org/10.1021/ic5018328 | Inorg. Chem. 2015, 54, 87−96

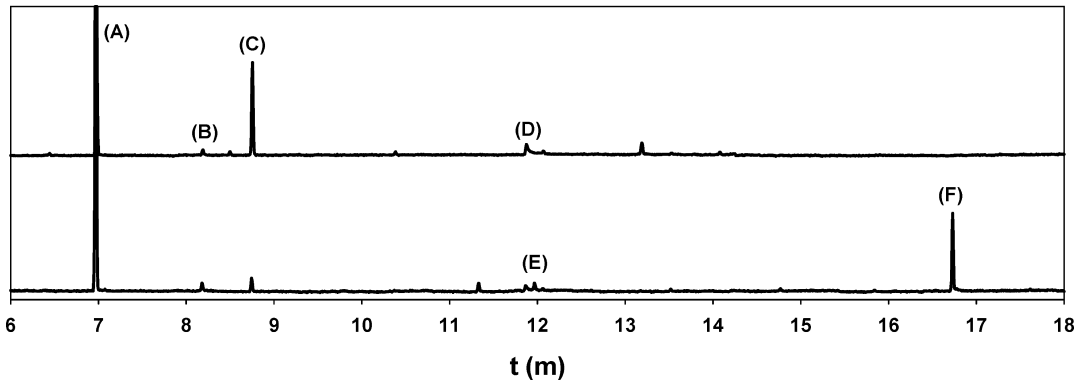

Figure 3. GC−MS data showing organic products from thermolysis of [(Tp^{Ph,Me})Ni−SMes] at 336 K in 1,2-dichloroethane with added MeI (0.5 M, top) and without (bottom). Peak labels: (A) naphthalene standard (m/z = 128), (B) MesSH (m/z = 152), (C) MeSMes (m/z = 166), (D) Hpz^{Ph,Me} (m/z = 158), (E) MesSCH$_2$CH$_2$Cl (m/z = 214), and (F) MesSSMes (m/z = 302).

$$[(\mathrm{Tp}^{R,Me})\mathrm{Ni{-}SAr}] + \mathrm{R'X} \rightarrow [(\mathrm{Tp}^{R,Me})\mathrm{Ni{-}X}] + \mathrm{R'SAr} \quad (1)$$

$$-\mathrm{d}[(\mathrm{Tp}^{R,Me})\mathrm{Ni{-}SAr}]/\mathrm{d}t = (k_0 + k_1[\mathrm{R'X}])[(\mathrm{Tp}^{R,Me})\mathrm{Ni{-}SAr}] \quad (2)$$

$$-\mathrm{d}[(\mathrm{Tp}^{R,Me})\mathrm{Ni{-}SAr}]/\mathrm{d}t = k_{obs}[(\mathrm{Tp}^{R,Me})\mathrm{Ni{-}SAr}] \quad (3)$$

where $k_{obs} = k_0 + k_1[\mathrm{R'X}]_0$ and $[\mathrm{R'X}]_0 \gg [(\mathrm{Tp}^{R,Me})\mathrm{Ni{-}SAr}]_0$

$$[(\mathrm{Tp}^{R,Me})\mathrm{Ni{-}SAr}] + \mathrm{ClCH_2CH_2Cl} \rightarrow [(\mathrm{Tp}^{R,Me})\mathrm{Ni{-}Cl}] + \mathrm{ArSCH_2CH_2Cl} \quad (4)$$

$$[(\mathrm{Tp}^{R,Me})\mathrm{Ni{-}SAr}] + \mathrm{H_2O} \rightarrow 1/n[(\mathrm{Tp}^{R,Me})\mathrm{Ni{-}OH}]_n + \mathrm{ArSH} \quad (5)$$

$$[(\mathrm{Tp}^{R,Me})\mathrm{Ni{-}SAr}] + \mathrm{O_2} \rightarrow [(\mathrm{Tp}^{R,Me})\mathrm{Ni}]^+ + \mathrm{O_2}^- + \frac{1}{2}\mathrm{ArSSAr} \quad (6)$$

3.2. Kinetics for Electrophilic Alkylation of [(Tp^{Ph,Me})-Ni−SMes]. Alkylation of [(Tp^{Ph,Me})Ni−SMes] with MeI was selected as the prototypical reaction because this reaction occurs on a convenient time scale near room temperature under pseudo-first-order conditions in nonpolar solvents (e.g., 100-fold excess MeI under argon in dry 1,2-dichloroethane) and is easily monitored by electronic spectroscopy (Figure 2). Conversion of the arylthiolate complex to [(Tp^{Ph,Me})Ni−I] is marked by an obvious bleaching of the reaction solution from dark purple to pale pink. Time-dependent UV−vis−NIR spectra at 326 K (Figure 2) showed a monotonic conversion to [(Tp^{Ph,Me})Ni−I] with bleaching of SAr → Ni ligand-to-metal charge-transfer (LMCT) bands and growth of the characteristic I → Ni LMCT bands (cf., Figure 1). A clear isosbestic point was maintained directly between these features at 461 nm; therefore, transient accumulation of any intermediate complex was not evident. Ligand field bands between 800 and 1100 nm sharpened with the increase in ideal point symmetry from C_s-[(Tp^{Ph,Me})Ni−SMes] to C_{3v}-[(Tp^{Ph,Me})Ni−I] but did not shift considerably, which is consistent with the comparable position of π-donating arylthiolates with respect to that of halides in the spectrochemical series.[61,62] Clean formation of the expected organosulfide coproduct MeSMes was previously demonstrated by ^{1}H NMR spectroscopy for alkylation of [(Tp^{Me,Me})Ni−SMes].[51] Given the expected overlap of the reactant and product arene resonances with the [(Tp^{Ph,Me})Ni−SMes] analogue, formation of the organosulfide coproduct MeSMes was alternatively confirmed by GC−MS measurements on the equilibrium solution (Figure 3).

The time-dependent absorption data were fit by global least-squares regression to the first-order integrated rate law to obtain the k_{obs} value (observed alkylation kinetics are compiled in Table S1 in the SI, and details of the global fitting analysis for the specific data shown in Figure 2 are given in Figures S1−S10 in the SI). Coincident results were obtained by least-squares fitting of exponentials to single-wavelength data at the maximal absorption change for both [(Tp^{Ph,Me})Ni−SMes] decay and [(Tp^{Ph,Me})Ni−I] accumulation (557 and 427 nm, respectively; Figure 2, inset). Kinetic behavior conforming to the overall second-order rate law (eq 2) was demonstrated by independently varying the initial concentrations of [(Tp^{Ph,Me})-Ni−SMes] and MeI at 308(1) K (Figure S11, SI). Linear least-squares regression of k_{obs} versus [MeI]$_0$ gave values of k_0 and k_1 from the intercept and slope, respectively (Figure 4 and Table S1 in the SI). Analyses of all other reactions involving a variety of arylthiolate complexes and organic electrophiles were conducted analogously (representative time-dependent spec-

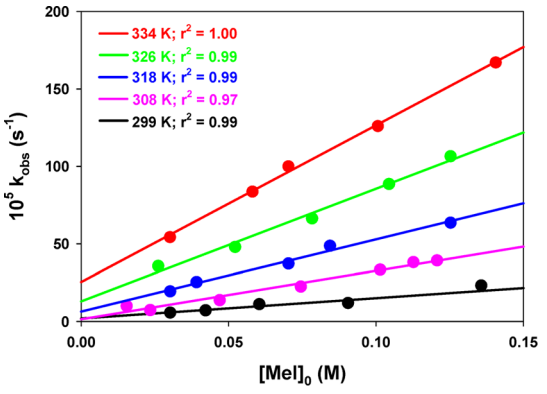

Figure 4. Plot of k_{obs} (s^{-1}) vs [MeI]$_0$ for alkylation of [(Tp^{Ph,Me})Ni−SMes] in 1,2-dichloroethane solution with linear least-squares regressions at the following temperatures: 299 K (black), k_0 = 2(1) × 10^{-5} s^{-1} and k_1 = 1.31(6) × 10^{-3} M^{-1} s^{-1}; 308 K (pink), k_0 = 1(2) × 10^{-5} s^{-1} and k_1 = 3.1(2) × 10^{-3} M^{-1} s^{-1}; 318 K (blue), k_0 = 6(2) × 10^{-5} s^{-1} and k_1 = 4.7(3) × 10^{-3} M^{-1} s^{-1}; 326 K (green), k_0 = 1.3(4) × 10^{-4} s^{-1} and k_1 = 7.3(5) × 10^{-3} M^{-1} s^{-1}; and 334 K (red), k_0 = 2.5(2) × 10^{-4} s^{-1} and k_1 = 1.01(3) × 10^{-2} M^{-1} s^{-1}.

dx.doi.org/10.1021/ic5018328 | Inorg. Chem. 2015, 54, 87−96

trophotometric data and pseudo-first-order fits are shown in Figures S12−S19 in the SI).

3.3. Arrhenius Behavior for Electrophilic Alkylation of [(Tp^{Ph,Me})Ni−SMes]. Observed reaction rates of [(Tp^{Ph,Me})Ni−SMes] were determined as a function of MeI concentration at five different temperatures between 299 and 334 K (Figure 4). A linear dependence of k_{obs} on $[MeI]_0$ was maintained at all temperatures, and Arrhenius plots were constructed for both the intercept and slope values (i.e., k_0 and k_1, respectively; Figure 5). Notwithstanding the volatility of MeI, both plots were linear and did not exhibit any obvious discontinuity. The minor k_0 pathway is a composite of reactions with halogenated solvent and adventitious O_2 (section 3.8 in the SI), and further consideration of the associated activation parameters is not warranted. Parameters calculated for the k_1 alkylation pathway were $\Delta H^{\ddagger}_{1,obs}$ = 11(1) kcal/mol and $\Delta S^{\ddagger}_{1,obs}$ = −37(4) cal mol^{-1} K^{-1}. Similar values were reported for electrophilic alkylations of several neutral Zn(II) complexes,[30−32,36] as well as square-planar and square-pyramidal Ni(II) (Table 1).[22,36,46] The small enthalpy and negative entropy are seemingly consistent with the bimolecular transition state of an S_N2 reaction mechanism; however, a dissociative mechanism was assigned to one of the zinc complexes, with solvent electrostriction proposed to account for the unfavorable entropy.[30]

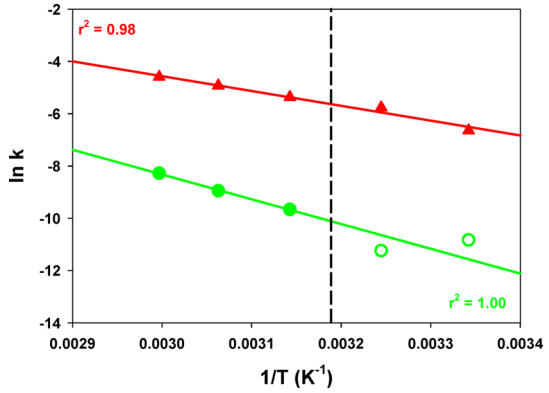

Figure 5. Arrhenius plot for k_0 (green, s^{-1}) and k_1 (red, M^{-1} s^{-1}) values for the reaction of MeI and [(Tp^{Ph,Me})Ni−SMes] in 1,2-dichloroethane using the respective intercepts and slopes fitted to the data in Figure 4. Open circles were not included in the linear regression to k_0 on the basis of a lack of statistical significance in the intercept values. The vertical dashed line represents the normal boiling point of MeI (1 atm).

3.4. Reaction of [(Tp^{Ph,Me})Ni−SMes] with Alternate Electrophiles. Reaction rates of [(Tp^{Ph,Me})Ni−SMes] with the alternative electrophiles benzyl bromide (Figure S12, SI) and ethyl iodide (data not shown) were also determined, but the elucidation of Arrhenius constants was constrained by the higher concentrations and temperatures required to obtain convenient reaction rates (Table S1, SI). Nevertheless, relative reactivities of the various electrophiles, including the contribution of 1,2-dichloroethane solvent to k_0 already described, can be compared using observed or interpolated k_1 values at 326 K: MeI (7.3(5) × 10^{-3} M^{-1} s^{-1}) > BzBr (3 × 10^{-4} M^{-1} s^{-1}) ≈ EtI (1.9(1) × 10^{-4} M^{-1} s^{-1}) > $ClCH_2CH_2Cl$ (≤1 × 10^{-5} M^{-1} s^{-1}). This trend is consistent with the participation of the R′X electrophiles in a common S_N2 reaction mechanism with respect to the order-of-magnitude kinetic effects induced by steric (R′: Me > Et)[40,47,63] and leaving group (X: I ≥ Br > Cl)[63] properties; however, the identity of the reactive nucleophile is not revealed by this comparison.

3.5. Solvent Effects for Electrophilic Alkylation of [(Tp^{Ph,Me})Ni−SMes]. Reaction of [(Tp^{Ph,Me})Ni−SMes] with MeI was determined near room temperature (299 K) in a range of other aprotic solvents (i.e., toluene, THF, $CHCl_3$, and CH_2Cl_2). These solvents were selected with the intention of varying the solvent polarity as much as possible while avoiding ionization of either the initial arylthiolate complex or the product halide complex. Time-dependent UV−vis−NIR spectra were comparable to those recorded in 1,2-dichloroethane, particularly with respect to the accumulation of

Table 1. Observed Activation Parameters for Bimolecular Electrophilic Reactions

nucleophile	geometry	electrophile	solvent	$\Delta H^{\ddagger}_{1,obs}$ (kcal/mol)	$\Delta S^{\ddagger}_{1,obs}$ (cal mol^{-1} K^{-1})	ref
[(L)Zn−SC$_6$H$_4$-2-NHC(O)^{t}Bu]^a	pseudo-T_d	BzBr	d^8-toluene	19(1)	−21(3)	31
[(L)Zn−SPh]^a	pseudo-T_d	BzBr	d^8-toluene	16(1)	−22(4)	31
[(L)Ni−SPh]^b	sq. planar	BzBr	d^8-toluene	14.7(2)	−32.3(7)	46
[(L^8)Ni−S−C$_6$H$_4$-4-Me]^c	sq. pyramid	BzBr	CH_3CN	10.3(7)	−32(2)	22
[(L)Zn−SPh]^a	pseudo-T_d	MeI	d^8-toluene	17(1)	−22(3)	31
[(Tm^{Ph})Zn−SCH$_2$C(O)NHPh]^d	pseudo-T_d	MeI	$CDCl_3$	14(1)	−23(4)	30
[(L1O)Zn−SBz]^e	pseudo-T_d	MeI	$CDCl_3$	8(2)	−35(6)	32
[(L)Zn]^f	pseudo-T_d	MeI	$CDCl_3$	12.9(7)	−27(3)	36
[(L)Ni]^f	sq. planar	MeI	$CDCl_3$	11(1)	−29(3)	36
[(Tp^{Ph,Me})Ni−SMes]	pseudo-T_d	MeI	$ClCH_2CH_2Cl$	11(1)	−37(4)	*g*
				$\Delta H^{\ddagger}_{7,obs}$ (kcal/mol)	$\Delta S^{\ddagger}_{7,obs}$ (cal mol^{-1} K^{-1})	
NEt_3		MeI	*n*-hexane	13.4(3)	−49(1)	67
NEt_3		MeI	benzene	8.5(3)	−52(1)	67
NEt_3		MeI	acetone	8.2(3)	−48(1)	67
NEt_3		EtI	acetone	11.6(2)	−38.8(5)	68

^{a}L = phenyl[3-*tert*-butyl-pyrazol-1-yl]bis[(*tert*-butylthio)methyl]borate. ^{b}L = κ^3-2,6-(OPPh$_2$)C$_6$H$_3$-1-ylate. ^{c}L^8 = 1,5-bis(2-pyridylmethyl)-1,5-diazacyclooctane. ^{d}Tm^{Ph} = hydrotris(2-mercapto-1-phenylimidazolyl)borate. ^{e}L1O = bis(3,5-dimethylpyrazol-1-yl)-6-(1-*tert*-butyl-4-methylphenolato)methane. ^{f}L = 6,6′-bis(2,2-diphenyl-2-ethylthiolato)-2,2′-bipyridine. ^{g}This Article.

dx.doi.org/10.1021/ic5018328 | Inorg. Chem. 2015, 54, 87−96

[(Tp^{Ph,Me})Ni−I] in the presence of excess MeI (data not shown). Linear correlations of k_{obs} to $[MeI]_0$ were observed in each solvent, and values of k_0 and k_1 were extracted as before (Figure 6).

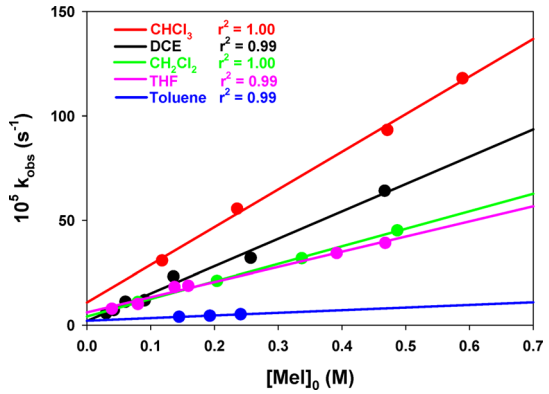

Figure 6. Plot of k_{obs} (s^{-1}) vs $[MeI]_0$ for alkylation of [(Tp^{Ph,Me})Ni−SMes] at 299 K with linear least-squares fits in the following solvents: $CHCl_3$ (red), $k_0 = 1.1(3) \times 10^{-4}$ s^{-1} and $k_1 = 1.80(7) \times 10^{-3}$ M^{-1} s^{-1}; 1,2-dichloroethane (black), $k_0 = 2(1) \times 10^{-5}$ s^{-1} and $k_1 = 1.31(6) \times 10^{-3}$ M^{-1} s^{-1}; CH_2Cl_2 (green), $k_0 = 4.1(4) \times 10^{-5}$ s^{-1} and $k_1 = 8.4(1) \times 10^{-4}$ M^{-1} s^{-1}; THF (pink), $k_0 = 6(1) \times 10^{-5}$ s^{-1} and $k_1 = 7.2(4) \times 10^{-4}$ M^{-1} s^{-1}; and toluene (blue), $k_0 = 2.1(3) \times 10^{-5}$ s^{-1} and $k_1 = 1.3(2) \times 10^{-4}$ M^{-1} s^{-1}.

Solvent medium effects for an S_N2 mechanism involving two neutral molecules is attributed to differing dipole interactions between solvent and solute molecules in the ground and transition states; an inverse logarithmic relationship between rate and the solvent dielectric (ε) is predicted, but the weak interaction and the contributions of other forces typically result in a poor correlation.[39] Such a correlation is somewhat evident in the present case ($r^2 = 0.67$, Figure 7) in which the negative slope implies charge accumulation in the transition state, consistent with an S_N2 mechanism. Further evidence for the accumulation of negative charge on the incipient iodide anion is

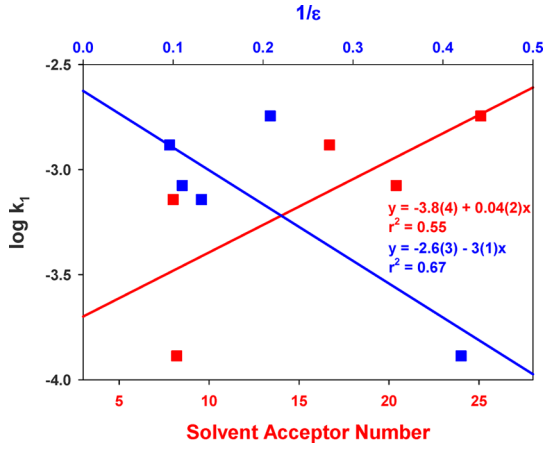

Figure 7. Plot of log k_1 (M^{-1} s^{-1}) for alkylation of [(Tp^{Ph,Me})Ni−SMes] with MeI at 299 K, obtained from the slopes shown in Figure 6, vs the inverse solvent dielectric constant (blue, upper horizontal axis) and Gutmann's solvent acceptor number (red, lower horizontal axis)[64] with linear least-squares fits. Because a solvent acceptor number has not been assigned for toluene, the value reported for benzene is used instead.

provided by positive correlation with Gutmann's solvent acceptor number ($r^2 = 0.55$, Figure 7).[64,65] A comparison can be made between the reaction of [(Tp^{Ph,Me})Ni−SMes] with MeI and the Menschutkin reaction of NEt_3 and EtI, which is the prototypical ionogenic bimolecular reaction of neutral polar molecules by an S_N2 mechanism (eq 7).[66] Comparison of k_1 at 299 K versus k_7 at 298 K in the same solvents reveals some correlation ($r^2 = 0.65$, Figure 8), suggesting a common

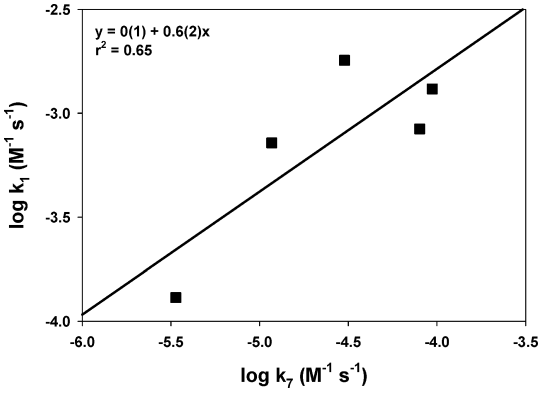

Figure 8. Correlation of the bimolecular rate constants k_1 for the reaction of [(Tp^{Ph,Me})Ni−SMes] with MeI, observed at 299 K in the various solvents shown in Figure 6, with k_7 for the reaction of Et_3N with EtI at 298 K in identical solvents.[66]

mechanism for the two reactions. A particular analogy is drawn between the product ion pair $[R'NEt_3]^+(X^-)$ and the putative associative intermediate $[(Tp^{R,Me})Ni(R'SAr)]^+(X^-)$ of interest herein (Scheme 1); covalent interaction between the incipient I^- and $[(Tp^{Ph,Me})Ni]^+$ ions in the transition state (i.e., σ-bond metathesis) has no analogy in the Menschutkin reaction, and a four-centered associative transition state is disfavored as a mechanistic feature in the reaction of [(Tp^{Ph,Me})Ni−SMes] on this basis.

$$Et_3N + EtI \rightarrow (NEt_4)^+I^- \quad (7)$$

A compensation effect is suggested by solvent-dependent activation parameters (Table 1),[39,67,68] in which reactions in more polar solvents tend to exhibit lower activation enthalpies and more negative activation entropies. Although the significance of such a correlation can be questioned,[69] a genuine compensation effect might arise through differential solvation of accumulating charge in the transition state.[69−72] In the alternative dissociative mechanism, k_1 would represent a composite of the pre-equilibrium and thiolate alkylation steps,[39] and the apparent solvent compensation would reflect some modulation of this convolution. In this event, the comparable reactivities of [(Tp^{Ph,Me})Ni−SMes] and NEt_3 would be coincidental.

3.6. Electronic Effects for Alkylation of [(Tp^{Ph,Me})Ni−S−C$_6$H$_4$-4-Y] with MeI. The kinetics for reaction of a series of complexes [(Tp^{Ph,Me})Ni−S−C$_6$H$_4$-4-Y] (Y = OMe, Me, H, Cl)[53] with MeI were determined at 298 K in 1,2-dichloroethane (Figures S13−S16, SI). Linear dependences of k_{obs} on $[MeI]_0$ were again found for all four complexes, with increasing slopes for the more electron-releasing substituents (Figure 9). A Hammett plot of k_1 against standard σ_p values yielded $\rho = -1.7(4)$ (Figure 10). In the context of an associative mechanism, the negative ρ value may reflect significant stabilization of positive charge accumulation on sulfur at the

dx.doi.org/10.1021/ic5018328 | Inorg. Chem. 2015, 54, 87−96

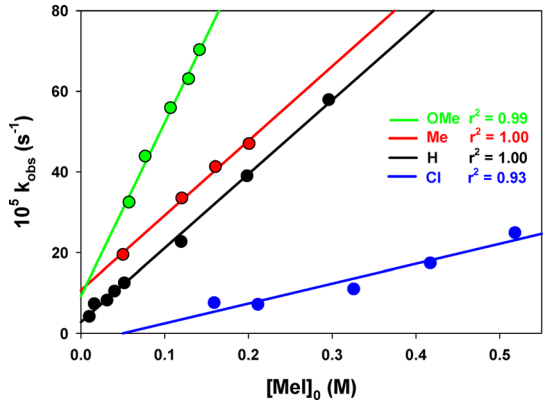

Figure 9. Plot of k_{obs} (s^{-1}) vs $[MeI]_0$ for alkylation of $[(Tp^{Ph,Me})Ni{-}S{-}C_6H_4\text{-}4\text{-}Y]$ in 1,2-dichloroethane at 298 K with linear least-squares fits: Y = OMe (green), $k_0 = 9(2) \times 10^{-5}$ s^{-1} and $k_1 = 4.3(2) \times 10^{-3}$ M^{-1} s^{-1}; Y = Me (red), $k_0 = 1.1(1) \times 10^{-4}$ s^{-1} and $k_1 = 1.85(9) \times 10^{-3}$ M^{-1} s^{-1}; Y = H (black), $k_0 = 2.8(6) \times 10^{-5}$ s^{-1} and $k_1 = 1.83(4) \times 10^{-3}$ M^{-1} s^{-1}; and Y = Cl (blue), $k_0 = -2(3) \times 10^{-5}$ s^{-1} and $k_1 = 4.9(8) \times 10^{-4}$ M^{-1} s^{-1}.

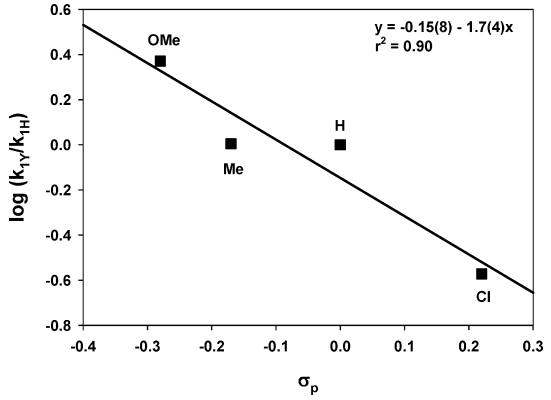

Figure 10. Hammett plot for reaction of $[(Tp^{Ph,Me})Ni{-}S{-}C_6H_4\text{-}4\text{-}Y]$ (Y = OMe, Me, H, Cl) with MeI in 1,2-dichloroethane at 298 K. Values of k_{1Y} are obtained from the slopes shown in Figure 9.

S_N2 transition state by electron-releasing substituents,[40,46] as well as ground-state destabilization of the reactive lone pair.[32] For example, a series of zinc complexes [(L1O)Zn−SR] (L1O = bis(3,5-dimethylpyrazol-1-yl)-6-(1-*tert*-butyl-4-methylphenolato)methane) was reacted with MeI in chloroform at 298 K, and a linear logarithmic correlation was found between the second-order observed rate constant and the aqueous pK_a of the free thiol, as well as an inverse correlation with the calculated HOMO energies of the thiolate complexes.[32] Our results also compare to $\rho = -1.8$ for alkylations of $[CpFe(CO)_2SAr]$ with MeI in acetone at 293 K[40] and to $\rho = -1.5$ for square-planar arylthiolate nickel(II) pincer complexes reacted with BzBr in toluene at 333 K.[46]

Two opposing effects would operate in a dissociative mechanism exhibiting second-order kinetics; a relatively electron-rich thiolate should exhibit less favorable dissociation, but would constitute a more potent nucleophile. The observed substituent effect would be a composite of these effects. In view of the larger ρ values observed for some nucleophilic substitutions,[39] this possibility cannot be excluded.

3.7. Substituent Effects for Reaction of $[(Tp^{R,Me})Ni{-}SAr]$ with MeI. To further elucidate the steric effects of proximal *o*-arylthiolate and 3-pyrazole substituents, we measured the rates of MeI alkylation over a range of arylthiolate complexes $[(Tp^{R,Me})Ni{-}S{-}2,4,6\text{-}R''_3C_6H_2]$ (R = Ph and R″ = H, Me, ^{i}Pr, or R = Me and R″ = H, ^{i}Pr). The data were obtained at 298−299 K (R = Ph: R″ = H, Figure S15, SI; Me, data not shown; ^{i}Pr, Figure S17, SI) or at 319 K (R = Me: R″ = H, Figure S18, SI; ^{i}Pr, Figure S19, SI) in 1,2-dichloroethane. The results afford some comparative insights into substituent effects.

For the series $[(Tp^{Ph,Me})Ni{-}S{-}2,4,6\text{-}R''_3C_6H_2]$, the trend observed at 298−299 K is a decrease in k_1 with increasing size of the arylthiolate substituent: R″ = H, $18.3(4) \times 10^{-4}$ M^{-1} s^{-1}; Me, $13.1(6) \times 10^{-4}$ M^{-1} s^{-1}; and ^{i}Pr, $7.6(9) \times 10^{-4}$ M^{-1} s^{-1} (Table S1 in the SI and Figure 11). Notwithstanding the

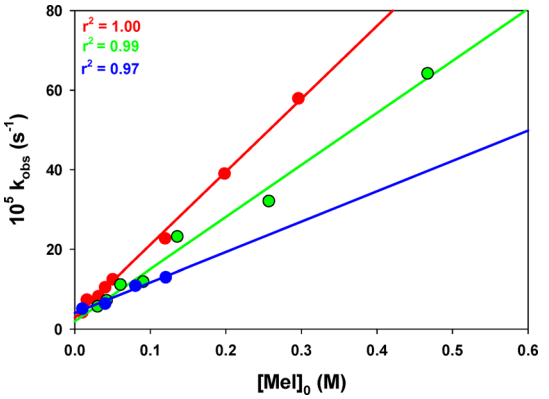

Figure 11. Plot of k_{obs} (s^{-1}) vs $[MeI]_0$ in 1,2-dichloroethane solutions for $[(Tp^{Ph,Me})Ni{-}SPh]$ at 298 K (red), $k_0 = 2.8(6) \times 10^{-5}$ s^{-1} and $k_1 = 1.83(4) \times 10^{-3}$ M^{-1} s^{-1}; $[(Tp^{Ph,Me})Ni{-}SMes]$ at 299 K (green), $k_0 = 2(1) \times 10^{-5}$ s^{-1} and $k_1 = 1.31(6) \times 10^{-3}$ M^{-1} s^{-1}; and $[(Tp^{Ph,Me})Ni{-}S{-}2,4,6\text{-}{}^iPr_3C_6H_2]$ at 298 K (blue), $k_0 = 4.1(7) \times 10^{-5}$ s^{-1} and $k_1 = 7.6(9) \times 10^{-4}$ M^{-1} s^{-1}.

electron-releasing properties of the added alkyl substituents, this trend suggests that ortho substituents may inhibit reactivity through a modest steric effect. The complexes just enumerated adopt a trigonal-pyramidal conformation with the arylthiolate substituent disposed between opposing pyrazole substituents.[53] Even with some rotation, the *o*-arylthiolate substituents are well positioned in this conformation to occlude the reactive sulfur lone pair from an approaching electrophile in an associative mechanism. In the alternative mechanism, dissociation of the more electron-rich thiolates would be less favorable.

The steric trend is inverted for less-reactive $[(Tp^{Me,Me})Ni{-}S{-}2,4,6\text{-}R''_3C_6H_2]$ analogues at 319 K as ortho substituents increase the rate of reaction: R″ = H, $4.4(4) \times 10^{-4}$ M^{-1} s^{-1}; ^{i}Pr, $7.3(6) \times 10^{-4}$ M^{-1} s^{-1} (Table S1 in the SI and Figure 12). Spectroscopic data indicate that $[(Tp^{Me,Me})Ni{-}S{-}2,4,6\text{-}{}^iPr_3C_6H_2]$ adopts a unique sawhorse conformation, in which the arylthiolate ring is disposed over a single 3-pyrazole methyl substituent and rotated 90° perpendicular to the Ni−S bond, displacing the ortho substituents away from the proximal electrophile; the Ni−SAr bond may also lengthen slightly, as observed between $[(Tp^{Me,Me})Ni{-}S{-}2,6\text{-}Ph_2C_6H_3]$ (2.2589(6) Å) and $[(Tp^{Me,Me})Ni{-}SPh]$ (2.2162(8) Å).[52] The greater reactivity of the substituted arylthiolate complex would reflect electronic effects in an associative mechanism, or more favorable arylthiolate dissociation in the sawhorse conformation, given a longer Ni−SAr bond.

Also noteworthy is the significant kinetic effect of the 3-pyrazole substituents. $[(Tp^{Ph,Me})Ni{-}SPh]$ exhibits four-fold

dx.doi.org/10.1021/ic5018328 | *Inorg. Chem.* 2015, 54, 87−96

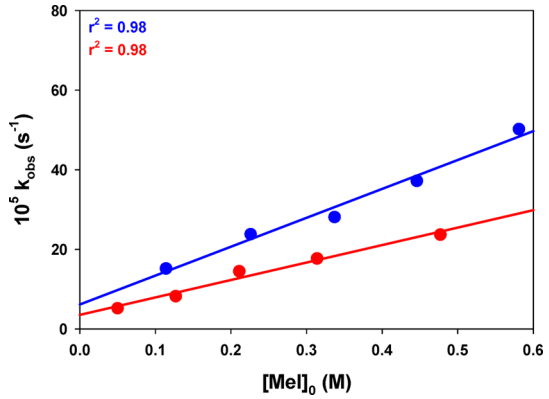

Figure 12. Plot of k_{obs} (s^{-1}) vs $[MeI]_0$ in 1,2-dichloroethane solutions at 319 K for $[(Tp^{Me,Me})Ni{-}SPh]$ (red), $k_0 = 4(1) \times 10^{-5}$ s^{-1} and $k_1 = 4.4(4) \times 10^{-4}$ M^{-1} s^{-1}; and $[(Tp^{Me,Me})Ni{-}S{-}2,4,6\text{-}{}^{i}Pr_3C_6H_2]$ (blue), $k_0 = 6(2) \times 10^{-5}$ s^{-1} and $k_1 = 7.3(6) \times 10^{-4}$ M^{-1} s^{-1}.

greater observed rates in comparison with those of $[(Tp^{Me,Me})Ni{-}SPh]$, notwithstanding a drop of 21 °C in temperature, which plausibly extrapolates to an order-of-magnitude difference under identical conditions. A comparable rate difference was observed in the zinc analogues $[(Tp^{R,Me})Zn{-}SAr]$ (R = Ph > R = Me), and the greater reactivity of the phenyl-substituted complex was tentatively ascribed to formation of a unique hydrophobic cavity around the arylthiolate coligand.[28] The comparison otherwise seems surprising in the context of an associative mechanism given that the sulfur atom should be more sterically accessible to electrophiles with smaller methyl substituents at the proximal 3-pyrazole positions. Overlooking minor differences in solvent and reaction temperature, reaction rates of MeI with $[(Tp^{Ph,Me})M{-}SPh]$ (M = Zn, Ni) are nearly identical (Zn, $2.0(1) \times 10^{-3}$ M^{-1} s^{-1} at 300 K in chloroform;[28] Ni, $1.83(4) \times 10^{-3}$ M^{-1} s^{-1} at 298 K in 1,2-dichloroethane), whereas the reaction of $[(Tp^{Ph,Ph})Zn{-}SPh]$ is modestly faster ($7(1) \times 10^{-3}$ M^{-1} s^{-1} in chloroform at 298 K).[32] The consistency of the observed rates for the Zn(II) analogues argues for a common mechanism, precluding an alternative redox pathway for the nickel complex.

A similar correspondence of observed rates was reported for reactions of the cationic square-pyramidal complexes incorporating a planar tetradentate pyridinane macrocyclic ligand $[(L^8)M{-}S{-}C_6H_4\text{-}4\text{-}Me](BPh_4)$ (M = Ni, Zn; L^8 = 1,5-bis(2-pyridylmethyl)-1,5-diazacyclooctane) with a fixed concentration of benzyl bromide in CD_3CN at 303 K.[22] On the basis of DFT calculations, it was proposed that destabilization of the filled and ligand-centered Ni−SAr σ^* orbital in Ni(II) offsets the greater anionic charge on sulfur in the Zn(II) complex, resulting in comparable nucleophilicity. Slower reactions were observed for iron(II) and cobalt(II) analogues, which is consistent with enhanced σ bonding arising from decreased occupancy of destabilized d orbitals. However, this argument does not clearly distinguish a reaction mechanism; enhanced M−SAr bonding would also suppress the rate of thiolate dissociation. An even greater kinetic effect was obtained for the pair of distorted square-planar complexes [(L)M] (M = Ni, Zn; L = κ^4-6,6′-bis(2,2-diphenyl-2-ethylthiolato)-2,2′-bipyridine) reacting with MeI in chloroform; in this geometry, the HOMO exhibits Ni−SAr π^* character, and the nickel complex is more reactive than the zinc analogue by nearly an order of magnitude.[36]

If we extend this argument, the rate enhancement observed for $[(Tp^{R,Me})Ni{-}SPh]$ (R = Ph > R = Me) might arise within an associative pathway partly as a result of increased Ni−SPh covalency at the expense of weaker tripodal scorpionate ligation in the presence of the larger 3-pyrazole phenyl substituents. Red-shifted ligand field bands observed in the corresponding halide complexes $[(Tp^{R,Me})Ni{-}Cl]$ (R = Me, Ph) are consistent with this proposal.[55,56] However, such an effect is not fully resolved in the X-ray crystal structures: Ni−N bond lengths range from 1.978(2)−1.992(2) Å for $[(Tp^{Me,Me})Ni{-}SPh]$ to 1.997(2)−2.019(2) Å for $[(Tp^{Ph,Me})Ni{-}SPh]$; the Ni−SAr bond lengths are coincident at 2.2162(8) and 2.2160(7)−2.2224(7) Å for these complexes, respectively.[51−53]

4. CONCLUSIONS

This study determined the kinetics for reactions of organic electrophiles R′X with pseudotetrahedral nickel(II) scorpionate complexes $[(Tp^{R,Me})Ni{-}SAr]$ (R = Me, Ph). Our results are intended to complement previous studies on zinc analogues,[28] as well as nickel(II) complexes in alternative square-planar and square-pyramidal geometries.[22,36,46,47] Our findings are briefly summarized as follows.

- Arylthiolate complexes $[(Tp^{R,Me})Ni{-}SAr]$ (R = Me, Ph) react with organic electrophiles R′X to form the free organosulfide R′SAr and the halide complex $[(Tp^{R,Me})Ni{-}X]$ without generation of observable complex intermediate(s);
- Observed kinetics conform to an overall second-order rate law, first-order each in complex and electrophile;
- The reaction rate accelerates in more polar solvents;
- The reaction rate increases for donating *p*-arylthiolate substituents in the isosteric series $[(Tp^{Ph,Me})Ni{-}S{-}C_6H_4\text{-}4\text{-}Y]$ (Y: Cl < H < Me < OMe);
- The reaction rate depends on the 3-pyrazole substituent and is generally greater for R = Ph than R = Me;
- Electron-donating *o*-arylthiolate alkyl substituents in $[(Tp^{R,Me})Ni{-}S{-}2,4,6\text{-}R''_3C_6H_2]$ (R″ = H, Me, ^{i}Pr) also enhance the rate for R = Me but inhibit the rate for R = Ph, which is consistent with differing conformational effects;[52,53]
- Observed rates for $[(Tp^{R,Me})Ni{-}SPh]$ (R = Me, Ph) are comparable to those of zinc analogues.[28]

The key mechanistic question concerns the identity of the reactive nucleophile, either the intact complex or a dissociated thiolate (Scheme 1). Reactions of $[(Tp^{R,Me})Ni{-}SAr]$ gave highly linear rate dependences on $[MeI]_0$ without obvious saturation. No direct evidence can be inferred for a dissociative mechanism, but neither is this precluded.[30] Therefore, we have elucidated a variety of kinetic and extrakinetic probes of mechanism to better constrain these possibilities. These phenomena include Arrhenius and Hammett analyses, as well as solvent and substituent effects. The large negative reaction entropy and moderate ρ value are consistent with an associative mechanism. Other correlations are more tenuous and limited in scope but may provide a fruitful subject for further investigation. Solvent effects, including a comparison to the Menschutkin reaction as well as a possible compensation effect, also provide evidence for an associative mechanism in the present study. Differential conformational effects of *o*-arylthiolate substituents observed for $[(Tp^{R,Me})Ni{-}S{-}2,4,6\text{-}R''_3C_6H_2]$ (R″ = H, Me, ^{i}Pr) are also consistent with reactions of intact complexes. An order-of-magnitude kinetic effect

dx.doi.org/10.1021/ic5018328 | Inorg. Chem. 2015, 54, 87−96

arising from 3-pyrazole ligand substituents was observed for [($Tp^{R,Me}$)Ni−SPh] (R = Me, Ph) complexes, as previously reported for zinc analogues.[28] Indeed, the enhanced covalency of the Ni−SAr bond exerts surprisingly little kinetic effect.[22,45]

In summary, although the entirety of our data is consistent with an associative mechanism involving intact thiolate complexes (Scheme 1, pathway C), some uncertainty remains. No single result definitively excludes a dissociative mechanism for electrophilic alkylation of neutral thiolate complexes in relatively nonpolar media. However, we have elucidated a rich array of kinetic phenomena for further investigation, including new conformational and solvent effects. Future work may provide additional mechanistic insights, promoting a better understanding of factors relevant for controlling biological methyltransferase reactivity.

■ ASSOCIATED CONTENT

Supporting Information

Tabulated kinetic data and miscellaneous spectroscopic and GC−MS data. This material is available free of charge via the Internet at http://pubs.acs.org.

■ AUTHOR INFORMATION

Corresponding Author

*E-mail: jensenm@ohio.edu.

Notes

The authors declare no competing financial interest.

■ ACKNOWLEDGMENTS

We acknowledge the donors of the American Chemical Society Petroleum Research Fund (49296-DNI3) for support of this research. We also thank the Ohio University 1804 Fund for support in acquiring the DFT computational facility.

■ REFERENCES

(1) Solomon, E. I.; Gorelsky, S. I.; Dey, A. *J. Comput. Chem.* **2006**, *27*, 1415−1428.
(2) Poulos, T. L. *Chem. Rev.* **2014**, *114*, 3919−3962.
(3) Sheng, Y.; Abreu, I. A.; Cabelli, D. E.; Maroney, M. J.; Miller, A.-F.; Teixeira, M.; Valentine, J. S. *Chem. Rev.* **2014**, *114*, 3854−3918.
(4) Yeh, A. P.; Hu, Y.; Jenney, F. E., Jr.; Adams, M. W. W.; Rees, D. C. *Biochemistry* **2000**, *39*, 2499−2508.
(5) Kovacs, J. A.; Brines, L. M. *Acc. Chem. Res.* **2007**, *40*, 501−509.
(6) Kovacs, J. A. *Chem. Rev.* **2004**, *104*, 825−848.
(7) Conrad, K. S.; Brunold, T. C. *Inorg. Chem.* **2011**, *50*, 8755−8766.
(8) Bouwman, E.; Reedijk, J. *Coord. Chem. Rev.* **2005**, *249*, 1555−1581.
(9) Can, M.; Armstrong, F. A.; Ragsdale, S. W. *Chem. Rev.* **2014**, *114*, 4149−4174.
(10) Ermler, U.; Grabarse, W.; Shima, S.; Goubeaud, M.; Thauer, R. K. *Science* **1997**, *278*, 1457−1462.
(11) Wilson, T. D.; Yu, Y.; Lu, Y. *Coord. Chem. Rev.* **2013**, *257*, 260−276.
(12) Parkin, G. *Chem. Rev.* **2004**, *104*, 699−768.
(13) Ferrer, J.-L.; Ravanel, S.; Robert, M.; Dumas, R. *J. Biol. Chem.* **2004**, *279*, 44235−44238.
(14) Mishina, Y.; Duguid, E. M.; He, C. *Chem. Rev.* **2006**, *106*, 215−232.
(15) Mathews, R. G.; Goulding, C. W. *Curr. Opin. Chem. Biol.* **1997**, *1*, 332−339.
(16) Szilagyi, R. K.; Bryngelson, P. A.; Maroney, M. J.; Hedman, B.; Hodgson, K. O.; Solomon, E. I. *J. Am. Chem. Soc.* **2004**, *126*, 3018−3019.
(17) Isaac, M.; Latour, J.-M.; Sénèque, O. *Chem. Sci.* **2012**, *3*, 3409−3420.
(18) Dey, A.; Jeffrey, S. P.; Darensbourg, M.; Hodgson, K. O.; Hedman, B.; Solomon, E. I. *Inorg. Chem.* **2007**, *46*, 4989−4996.
(19) Penner-Hahn, J. *Curr. Opin. Chem. Biol.* **2007**, *11*, 166−171.
(20) Wilker, J. J.; Lippard, S. J. *J. Am. Chem. Soc.* **1995**, *117*, 8682−8683.
(21) Wilker, J. J.; Lippard, S. J. *Inorg. Chem.* **1997**, *36*, 969−978.
(22) Fox, D. C.; Fiedler, A. T.; Halfen, H. L.; Brunold, T. C.; Halfen, J. A. *J. Am. Chem. Soc.* **2004**, *126*, 7627−7638.
(23) Notni, J.; Günther, W.; Anders, E. *Eur. J. Inorg. Chem.* **2007**, 985−993.
(24) Trofimenko, S. *Chem. Rev.* **1993**, *93*, 943−980.
(25) Brand, U.; Rombach, M.; Vahrenkamp, H. *Chem. Commun. (Cambridge, U.K.)* **1998**, 2717−2718.
(26) Brand, U.; Rombach, M.; Seebacher, J.; Vahrenkamp, H. *Inorg. Chem.* **2001**, *40*, 6151−6157.
(27) Ji, M.; Benkmil, B.; Vahrenkamp, H. *Inorg. Chem.* **2005**, *44*, 3518−3523.
(28) Rombach, M.; Seebacher, J.; Ji, M.; Zhang, G.; He, G.; Ibrahim, M. M.; Benkmil, B.; Vahrenkamp, H. *Inorg. Chem.* **2006**, *45*, 4571−4575.
(29) Bridgewater, B. M.; Fillebeen, T.; Friesner, R. A.; Parkin, G. *J. Chem. Soc., Dalton Trans.* **2000**, 4494−4496.
(30) Morlok, M. M.; Janak, K. E.; Zhu, G.; Quarless, D. A.; Parkin, G. *J. Am. Chem. Soc.* **2005**, *127*, 14039−14050.
(31) Chiou, S.-J.; Riordan, C. G.; Rheingold, A. L. *Proc. Natl. Acad. Sci. U.S.A.* **2003**, *100*, 3695−3700.
(32) Warthen, C. R.; Hammes, B. S.; Carrano, C. J.; Crans, D. C. *JBIC, J. Biol. Inorg. Chem.* **2001**, *6*, 82−90.
(33) Hammes, B. S.; Carrano, C. J. *Chem. Commun. (Cambridge, U.K.)* **2000**, 1635−1636.
(34) Hammes, B. S.; Carrano, C. J. *Inorg. Chem.* **2001**, *40*, 919−927.
(35) Grapperhaus, C. A.; Tuntulani, T.; Reibenspies, J. H.; Darensbourg, M. Y. *Inorg. Chem.* **1998**, *37*, 4052−4058.
(36) Gennari, M.; Retegan, M.; DeBeer, S.; Pécaut, J.; Neese, F.; Collomb, M.-N.; Duboc, C. *Inorg. Chem.* **2011**, *50*, 10047−10055.
(37) Picot, D.; Ohanessian, G.; Frison, G. *Inorg. Chem.* **2008**, *47*, 8167−8178.
(38) Pearson, R. G.; Sobel, H. R.; Songstad, J. *J. Am. Chem. Soc.* **1968**, *90*, 319−326.
(39) Espenson, J. H. *Chemical Kinetics and Reaction Mechanisms*, 2nd ed.; McGraw-Hill: New York, 1995.
(40) Ashby, M. T.; Enemark, J. H.; Lichtenberger, D. L. *Inorg. Chem.* **1988**, *27*, 191−197.
(41) King, R. B.; Bisnette, M. B. *Inorg. Chem.* **1965**, *4*, 482−485.
(42) Schumann, H.; Arif, A. M.; Rheingold, A. L.; Janiak, C.; Hoffmann, R.; Kuhn, N. *Inorg. Chem.* **1991**, *30*, 1618−1625.
(43) Boerzel, H.; Koeckert, M.; Bu, W.; Spingler, B.; Lippard, S. J. *Inorg. Chem.* **2003**, *42*, 1604−1615.
(44) Melnick, J. G.; Zhu, G.; Buccella, D.; Parkin, G. *J. Inorg. Biochem.* **2006**, *100*, 1147−1154.
(45) Gorelsky, S. I.; Basumallick, L.; Vura-Weis, J.; Sarangi, R.; Hodgson, K. O.; Hedman, B.; Fujisawa, K.; Solomon, E. I. *Inorg. Chem.* **2005**, *44*, 4947−4960.
(46) Zhang, J.; Adhikary, A.; King, K. M.; Krause, J. A.; Guan, H. *Dalton Trans.* **2012**, *41*, 7959−7968.
(47) Ram, M. S.; Riordan, C. G.; Ostrander, R.; Rheingold, A. L. *Inorg. Chem.* **1995**, *34*, 5884−5892.
(48) MacBeth, C. E.; Thomas, J. C.; Betley, T. A.; Peters, J. C. *Inorg. Chem.* **2004**, *43*, 4645−4662.
(49) Cho, J.; Yap, G. P. A.; Riordan, C. G. *Inorg. Chem.* **2007**, *46*, 11308−11315.
(50) Van Heuvelen, K. M.; Cho, J.; Dingee, T.; Riordan, C. G.; Brunold, T. C. *Inorg. Chem.* **2010**, *49*, 6535−6544.
(51) Chattopadhyay, S.; Deb, T.; Ma, H.; Petersen, J. L.; Young, V. G., Jr.; Jensen, M. P. *Inorg. Chem.* **2008**, *47*, 3384−3392.
(52) Chattopadhyay, S.; Deb, T.; Petersen, J. L.; Young, V. G., Jr.; Jensen, M. P. *Inorg. Chem.* **2010**, *49*, 457−467.
(53) Deb, T.; Anderson, C. M.; Chattopadhyay, S.; Ma, H.; Young, V. G., Jr.; Jensen, M. P. *Dalton Trans.* **2014**, *43*, 17489−17499.

(54) Nakazawa, J.; Ogiwara, H.; Kashiwazaki, Y.; Ishii, A.; Imamura, N.; Samejima, Y.; Hikichi, S. *Inorg. Chem.* **2011**, *50*, 9933−9935.
(55) Desrochers, P. J.; Telser, J.; Zvyagin, S. A.; Ozarowski, A.; Krzystek, J.; Vicic, D. A. *Inorg. Chem.* **2006**, *45*, 8930−8941.
(56) Deb, T.; Anderson, C. M.; Ma, H.; Petersen, J. L.; Young, V. G., Jr.; Jensen, M. P. *Eur. J. Inorg. Chem.* **2014**, accepted.
(57) Deb, T.; Rohde, G. T.; Young, V. G., Jr.; Jensen, M. P. *Inorg. Chem.* **2012**, *51*, 7257−7270.
(58) *SPECFIT/32*, version 3.0; Spectrum Software Associates: Marlborough, MA, 2005.
(59) Maeder, M.; Zuberbühler, A. D. *Anal. Chem.* **1990**, *62*, 2220−2224.
(60) *SigmaPlot*, version 8.02; SPSS, Inc.: Chicago, 2001.
(61) Hollebone, B. R.; Nyholm, R. S. *J. Chem. Soc. A* **1971**, 332−337.
(62) Lane, R. W.; Ibers, J. A.; Frankel, R. B.; Papaefthymiou, G. C.; Holm, R. H. *J. Am. Chem. Soc.* **1977**, *99*, 84−98.
(63) Carey, F. A.; Sundberg, R. J. *Advanced Organic Chemistry*, 2nd ed., Part A; Plenum: New York, 1984.
(64) Mayer, U.; Gutmann, V.; Gerger, W. *Monatsh. Chem.* **1975**, *106*, 1235−1257.
(65) Gutmann, V. *Electrochim. Acta* **1976**, *21*, 661−670.
(66) Abraham, M. H.; Grellier, P. L. *J. Chem. Soc., Perkin Trans. 2* **1976**, 1735−1741.
(67) Brauer, H.-D.; Kelm, H. *Z. Phys. Chem. (Muenchen, Ger.)* **1971**, *76*, 98−107.
(68) Brauer, H.-D.; Kelm, H. *Z. Phys. Chem. (Muenchen, Ger.)* **1972**, *79*, 96−102.
(69) Liu, L.; Guo, Q.-X. *Chem. Rev.* **2001**, *101*, 673−696.
(70) Solà, M.; Lledós, A.; Duran, M.; Bertrán, J.; Abboud, J.-L. M. *J. Am. Chem. Soc.* **1991**, *113*, 2873−2879.
(71) Acevedo, O.; Jorgensen, W. L. *J. Phys. Chem. B* **2010**, *114*, 8425−8430.
(72) Shaik, S.; Ioffe, A.; Reddy, A. C.; Pross, A. *J. Am. Chem. Soc.* **1994**, *116*, 262−273.
(73) Roberts, J. L., Jr.; Sawyer, D. T. *J. Am. Chem. Soc.* **1981**, *103*, 712−714.